EPRI | ELECTRIC POWER RESEARCH INSTITUTE

Program on Technology Innovation: Coastal Halogen Atmospheric Research on Mercury Deposition (CHARMeD)

Program on Technology Innovation: Coastal Halogen Atmospheric Research on Mercury Deposition (CHARMeD)

1019522

Interim Report, August 2009

Cosponsor
University of Colorado at Boulder
Department of Chemistry & Biochemistry
Campus Box 215
Boulder, Colorado 80309-0215

Project Manager
R. M. Volkamer

EPRI Project Manager
A. ter Schure

ELECTRIC POWER RESEARCH INSTITUTE
3420 Hillview Avenue, Palo Alto, California 94304-1338 • PO Box 10412, Palo Alto, California 94303-0813 • USA
800.313.3774 • 650.855.2121 • askepri@epri.com • www.epri.com

DISCLAIMER OF WARRANTIES AND LIMITATION OF LIABILITIES

ORGANIZATION(S) THAT PREPARED THIS DOCUMENT

University of Colorado at Boulder, Department of Chemistry & Biochemistry

NOTE

CITATIONS

This report was prepared by

University of Colorado at Boulder
Department of Chemistry & Biochemistry
Campus Box 215
Boulder, Colorado 80309-0215

Principal Investigator
R. M. Volkamer

This report describes research sponsored by the Electric Power Research Institute (EPRI) and the University of Colorado at Boulder.

The report is a corporate document that should be cited in the literature in the following manner:

Program on Technology Innovation: Coastal Halogen Atmospheric Research on Mercury Deposition (CHARMeD). EPRI, Palo Alto, CA and the University of Colorado, Boulder, CO: 2009. 1019522.

PRODUCT DESCRIPTION

Determining mercury's atmospheric transformation reactions is essential for atmospheric deposition models that are used for regulatory purposes. It is the oxidation of inorganic elemental Hg (Hg^0) to its water-soluble ionic form (Hg^{2+}) that determines the rate of Hg deposited in waterways. Substantial research has been done in the past on atmospheric Hg transformation reactions with ozone (O_3) and the hydroxyl radical (OH), but O_3 and OH may not be capable of fully causing mercury's observed oxidation and subsequent measured wet deposition patterns in the United States. For example, in Florida and along the Gulf Coast there are few mercury sources; but the measured mercury wet deposition and concentrations are higher than anywhere else in the United States. Halogens, such as bromine oxide (BrO) and iodine oxide (IO), are suspected to play a role in mercury oxidation in such coastal areas. EPRI funded a study through its Innovator Circle program to study the importance of mercury oxidation by halogens on the measured enhanced wet deposition and concentrations in the southeastern United States.

Results and Findings

BrO and IO measurements conducted at the Southeastern Aerosol Research and Characterization Network (SEARCH) site Outlying Landing Field #8 (OLF) in Pensacola, Florida between March and November of 2008 showed concentrations below the detection limits of <5ppt for BrO and <2ppt for IO during most of this time.

A numerical box-model indicated that more than 99% of chemically active forms of bromine are converted into chemically inert reservoir species within a minute. BrO cannot survive transport from the coast to the 15km inland site, which typically takes about an hour. Conversion of BrO to inert species can occur by formaldehyde (HCHO) and glyoxal (CHOCHO); these compounds were measured at 1.5ppb for HCHO and 0.15ppb for CHOCHO at the site. Halogen oxide measurements require a more sensitive instrument at a site with lower influence of such efficient chemical sinks for bromine.

Challenges and Objectives

The reasons for the measured high mercury wet deposition and concentrations in Florida and along the Gulf Coast are currently not well understood. Since there are few mercury sources in these areas, the mercury deposition patterns are clearly not determined by proximity to sources alone, but by atmospheric chemical transformation and subsequent removal processes as well. The presence, rate, and ubiquity of these processes must be demonstrated in coastal environments to elucidate observed mercury deposition patterns. The work described here tests whether and to what extent halogen-mediated mercury oxidation reactions occur in the marine boundary layer along the coastal regions of the southeastern United States. The research will expand our understanding of how mercury sources relate to overall wet deposition.

Applications, Values, and Use

The linking of mercury atmospheric sources and its wet deposition to receptors requires the use of atmospheric physicochemical models. Current models inadequately simulate chemical processes in the coastal atmosphere, causing a discrepancy between measured and modeled wet deposition. A key removal process for mercury from the atmosphere is oxidation of elemental mercury to its ionized form. The oxidation of Hg^0 is currently represented in atmospheric models by reactions with O_3 and OH. However, it seems that O_3 and OH may not be capable of fully causing mercury's observed oxidation while the BrO and IO abundant in coastal air could. Establishing whether potentially rapid and complete mercury oxidation reactions occur in coastal environments by halogens will allow model improvements that better simulate the contributions of mercury atmospheric sources to overall wet deposition, thus allowing a better fit between model outcomes and actual processes in the atmosphere and a more realistic allocation of deposited mercury to its sources.

EPRI Perspective

This report describes a first-of-a-kind study that attempts to elucidate the observed elevated mercury wet deposition rates and concentrations along the south eastern United States by measuring halogens, speciated mercury, and other air constituents. The work done at the SEARCH network site OLF is a fundamental contribution to understanding whether halogens drive the oxidation of elemental to divalent mercury in the coastal atmosphere, thereby partly explaining the observed deposition rates. The measured concentrations of chemical species and the reactions they imply may substantially alter our understanding of the relative contribution of nearby and distant sources to Hg deposition patterns.

Approach

The project team deployed a mini multi axis differential optical absorption spectroscope (MAX-DOAS) at the SEARCH network site OLF. The site is equipped with an automated speciated Tekran ambient Hg monitor, which measures Hg^0, reactive gas mercury, and particulate mercury, as well as instruments to measure key atmospheric constituents, such as O_3, SO_3, SO_2, $PM_{2.5}$, and meteorological parameters, such as wind speed and direction, temperature, and humidity. The team operated the mini-MAX-DOAS between March and November of 2008 to determine levels of bromine oxide (BrO), iodine oxide (IO), HCHO, CHOCHO, and other species. To determine the relevance of sink reactions, the team developed a photochemical box model to illustrate the effect that elevated concentrations of such constituents such as HCHO and CHOCHO may have on removing reactive halogens from the atmosphere.

Keywords

Mercury	Halogens
Air Toxics	Atmosphere
Atmospheric Chemistry	Modeling
Bromine Oxide	Iodine Oxide
MAX-DOAS	SEARCH

OVOCs (oxygenated volatile organic compounds)

ABSTRACT

The atmospheric oxidation of elemental mercury (Hg^0) is important because it produces reactive gaseous mercury (RGM) that rapidly deposits back on the Earth's surface and thus is an important source of mercury in water bodies, where it can be converted through natural biological reactions to the neurotoxin methyl mercury that enters the food chain through bioaccumulation in fish. This is a problem, particularly in the southeastern United States in Florida and along the Gulf Coast, where mercury deposition rates are up to five times higher than in the rest of the United States. The reasons for this high deposition are currently not well understood. One school of thought is that although ozone (O_3) and hydroxyl radicals (OH) may not be capable of fully causing the observed levels of mercury oxidation, the halogens bromine (Br) and iodine (I) that are more abundant in coastal air could be. A first attempt was made to measure the oxygenated halogen species BrO and IO in the coastal atmosphere of the Gulf coast. The concentration of BrO concentrations is typically 1-2 orders of magnitude larger than the concentration of Br atoms, and observations of BrO thus provides a very sensitive means to infer Br atom concentrations. A Multi AXis Differential Optical Absorption Spectroscopy (MAX-DOAS) instrument was used to measure halogen oxide radicals at a coastal/rural site located 21km north of the Gulf Coast near Pensacola, Florida. MAX-DOAS uses scattered solar light to directly measure atmospheric trace gases in the atmosphere without the need to pull air through sampling lines. A telescope collects scattered light at a series of different viewing angles above the horizon, and the integrated concentrations of trace gases along each line of sight is derived. The instrument was operated between March and November 2008 resulting in over 100 days of measurements. All spectra were analyzed for bromine oxide (BrO), iodine oxide (IO), nitrogen dioxide (NO_2), and oxygen dimers (O_4). The oxygenated volatile organic compounds (OVOC) formaldehyde (HCHO) and glyoxal (CHOCHO) were also analyzed. HCHO and CHOCHO present efficient sinks for bromine and are therefore important to measure conjunctively. Typical HCHO concentrations were 1.5 ppb and CHOCHO concentrations were 0.15ppb. BrO and IO concentrations were below the detection limits of <5ppt for BrO and <2ppt for IO in virtually all cases. A numerical box-model, using supplementary data collected at the site, reveals that more than 99% of chemically active forms of bromine are converted into chemically inert reservoir species within a minute. Thus BrO cannot survive transport from the coast to the site, which typically takes about 1hr. Useful halogen oxide measurements near Pensacola, Florida will require a site with lower influence of efficient chemical-sinks for bromine. Attempts to measure halogen oxides with a more sensitive instrument are now underway at a site <0.5 miles from the Gulf Coast.

ACKNOWLEDGMENTS

This work would not have been possible without the efforts of many people. The authors would like to acknowledge the following people.

For their direction and leadership, recognition is given to Arnout Ter Schure and Leonard Levin of EPRI.

At the University of Colorado, Boulder, thanks go to all members of the Atmospheric Trace Molecule Spectroscopy Laboratory (ATMOSpeclab, the PI's research group), in particular Sean Coburn, Dr. Barbara Dix and Dr. Roman Sinreich.

We would also like to thank the other EPRI contractors who contributed to the effort, including Eric Edgerton from ARA Inc.

Last, special thanks are expressed to the Integrated Instrument Development Facility of the Cooperative Institute for Research in Environmental Sciences (CIRES) at the University of Colorado at Boulder for help with machining parts to refurbish the Mini MAX-DOAS instrument.

NOMENCLATURE

μg	microgram (10^{-6} grams)
Br	bromine, atoms
Br_2	bromine, molecular
$BrNO_2$	bromine nitrite
BrO	bromine oxide
$BrONO_2$	bromine nitrate
CHOCHO	glyoxal
ClO	chlorine oxide
dSCD	differential slant column density
GEM	gaseous elemental mercury
HBr	hydrogen bromide
HCHO	formaldehyde
Hg	mercury
Hg^0	elemental mercury
Hg^{2+}	oxidized mercury
HgBr	mercury bromide
HgO	mercury oxide
HgOH	mercury hydrogen oxide
HgP	particulate mercury
HO_2	hydroperoxyl radical
HOBr	bromine hydrogen oxide
hν	sun light
I	iodine
IO	iodine oxide
masl	meters above sea level
MAX-DOAS	multi axis differential optical absorption spectroscopy
MDE	mercury depletion events
ng	nanogram (10^{-9} grams)
nm	nanometer (10^{-9} meters)
NO	nitrogen oxide
NO_2	nitrogen dioxide (nitrite)
NO_x	nitrogen oxides (sum of NO and NO_2)
O_2	oxygen
O_4	oxygen dimers
OH	hydroxyl radical
OLF	Outlying Landing Field #8
OVOC	oxygenated volatile organic compounds
pg	picogram (10^{-12} grams)
$PM_{2.5}$	fine particulate matter (2.5 micrometers in diameter and smaller)

ppb	parts per billion (10^{-9} volume mixing ratio)
ppt	parts per trillion (10^{-12} volume mixing ratio)
RGM	reactive gas mercury
SCD	slant column density (molecules cm^{-2})
SEARCH	southeastern aerosol research and characterization network
WDR	wind direction
WSP	wind speed

CONTENTS

LIST OF FIGURES

LIST OF TABLES

1
INTRODUCTION

Mercury (Hg) in the environment originates from both natural and anthropogenic sources. Natural sources include soils, vegetation, volcanoes, fires, and mineral deposits. Anthropogenic sources are coal combustion, waste incineration, and chlor-alkali production among others; about 2/3 of the total global mercury is believed of anthropogenic origin[1]. The atmospheric oxidation of gaseous elemental mercury (GEM: Hg^0) is important because it produces reactive gaseous mercury (RGM: Hg^{2+}) that rapidly deposits in the environment. RGM deposition is often the major source for mercury to water bodies, where RGM can be converted through natural biological reactions to the neurotoxin methyl mercury and enters the food chain via bioaccumulation in fish. This is a problem in particular in the southeastern United States, in Florida and along the Gulf Coast, where measured deposition rates of mercury are 2-5 times higher than in for example Pennsylvania and Ohio (Figure 1-1)[2, 3]. The reasons for this high deposition are currently not well understood; there are few mercury sources in Florida and along the Gulf Coast, but there are many sources, such as coal-fired power plants in Pennsylvania and Ohio. Clearly, the mercury deposition patterns are not only determined by proximity to sources, but by atmospheric chemical transformation and removal processes as well.

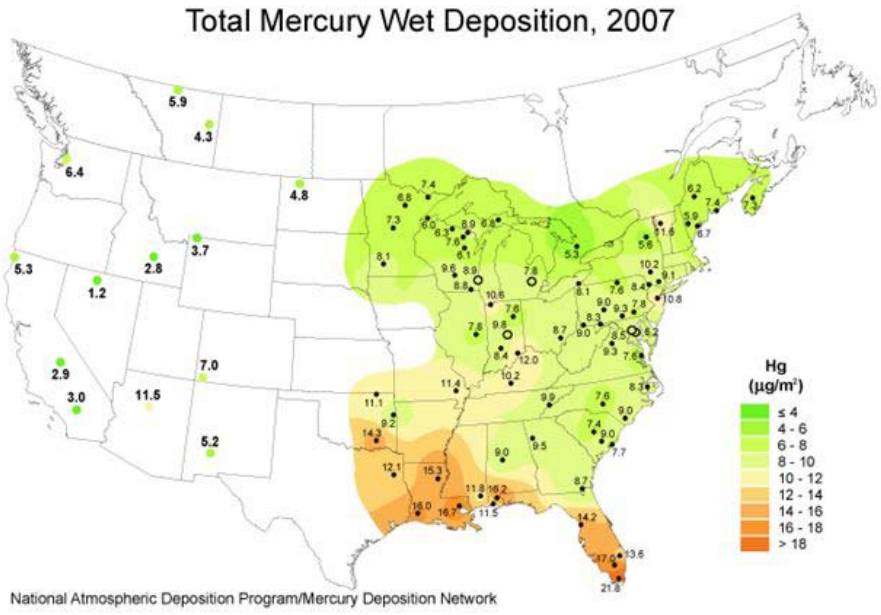

Figure 1-1
National Atmospheric Deposition Program/Mercury Deposition Network (NADP/MDN) deposition map for total mercury (µg m^{-2}) in 2007. Available at http://nadp.sws.uiuc.edu/mdn/maps/

A key removal process for mercury from the atmosphere is oxidation of Hg^0 to RGM. However, it seems that ozone (O_3) and hydroxyl radicals (OH) may not be capable of fully causing mercury's observed oxidation whereas halogens -bromine (Br) and iodine (I)- that are especially abundant in coastal air could.

The oxidation of Hg^0 is currently represented in atmospheric models only by reactions with ozone (R1) and the hydroxyl radical (R2)[4]. However, various reactions between Hg^0 and different bromine species have been proposed and studied[5, 6, 7, 8]. The reaction most likely to make significant contributions to the conversion of Hg^0 to RGM is the reaction with atomic bromine, Br (R3).

(R1) $Hg^0 + O_3 \rightarrow HgO + O_2$ $\quad k = 7.5 \times 10^{-19}$ cm^3 molecule^{-1} s^{-1}

(R2a) $Hg^0 + OH \rightarrow HgO + H$

(R2b) $Hg^0 + OH + M \rightarrow HgOH$ $\quad k \approx 1 \times 10^{-14}$ cm^3 molecule^{-1} s^{-1}

(R3) $Hg^0 + Br + M \rightarrow HgBr + M$ $\quad k = 3.2 \times 10^{-12}$ cm^3 molecule^{-1} s^{-1}

(R4) $HgBr + Br \rightarrow Hg^0 + Br_2$ $\quad k = 9.6 \times 10^{-11}$ cm^3 molecule^{-1} s^{-1}

The rate coefficient for (R1) is currently being debated; measurements vary from 6.4×10^{-19} to 3×10^{-20} cm^3 molecule^{-1} s^{-1}. By using the most recently published rate of reaction ($k_{R1} = 7.5 \times 10^{-19}$ cm^3 molecule^{-1} s^{-1})[9], and a typical tropospheric ozone concentrations at sea level, 1012 molecules cm^{-3} (~40 ppb), a Hg^0 half-life against oxidation by ozone is estimated at about 11 days. Such a short lifetime is unrealistic as it produces predicted surface concentrations of Hg^0 that are much lower than observations[5]. Additionally, the strong diurnal cycle of RGM seen by measurements is difficult to reconcile with ozone as the main oxidant, because ozone does not exhibit a very strong diurnal cycle[5]. Additionally, both (R1) and (R2a) depend on the formation of HgO, the binding energy of which is currently disputed; based on recent evidence both reactions might be endothermic and produce positive free energies.[10] In addition, two different thermodynamic studies found the binding energy of HgOH between 30 – 40 kJ mol^{-1}, hence HgOH will rapidly thermally dissociate at room temperature[5]. Based on the evidence above, the relevance of (R1) and (R2a,b) have likely been overestimated. However, thermodynamic calculations indicate that (R3) is an energetically favorable reaction[8]. Measured rate coefficients span from 3.2×10^{-12} to 3.6×10^{-13} cm^3 molecule^{-1} s^{-1} [6,7]. Assuming a concentration of Br radicals of ~2.5×10^5 molec cm^{-3} (~0.01 ppt)[3], the half-life of Hg^0 against oxidation by Br ranges from 10 – 90 days. These half-lives are within reason for Br to be the major oxidative pathway for Hg^0. In addition, since Br is photolytically produced, oxidation through this mechanism could explain the observed diurnal cycle of RGM. In the Arctic atmosphere observations have linked periods of elevated halogen oxide concentrations to mercury depletion events (MDE) during polar spring. Similar chemistry has been observed to be operative at the Dead Sea[11, 12, 13]. The extent to which these observations are relevant for the mid-latitude marine boundary layer is presently not clear.

During the day Br is in a rapid equilibrium with BrO: Br reacts rapidly with ozone, which is ubiquitous in the atmosphere, via (R5, see Section 2) to form BrO; BrO rapidly photolyzes ($\tau_{phot, BrO}$ = 100 sec), and can react with NO, BrO, IO, ClO to recycle Br atoms (see below). Owing to

the longer lifetime of BrO compared with Br ($\tau_{BrO} \leq 100$ sec during the day, compared to τ_{Br} = 0.8sec for [O_3] = 40ppb), the BrO concentration is typically 1-2 orders of magnitude larger than that of Br atoms. Observations of BrO thus provide very sensitive means to infer Br atom concentrations. The BrO/Br ratio is a function of environmental conditions: it tends to be higher at lower NO_x and can also be affected by NO_2, and HO_2 which react with BrO and Br to form chemically inert reservoir (long-lived) species of bromine. Br atoms also readily react with oxygenated hydrocarbons like formaldehyde (HCHO) and glyoxal (CHOCHO) to form HBr. This pathway effectively removes active forms of halogens from the atmosphere.

In the past, the well-established Differential Optical Absorption Spectroscopy (DOAS) technique has been used to measure halogen oxides[14, 15]. Multi-AXis (MAX) DOAS is a relatively young analytical technique that uses scattered solar light to measure atmospheric trace gases directly in the atmosphere (without pulling air through any sampling lines which could remove halogen oxides by deposition on the tubing or reactions with the tubing). It is based on the principal that trace gases in the atmosphere absorb sunlight differently. The analyzer detects each gas by measuring the different absorption profiles through a telescope that collects scattered light at a series of different viewing angles above the horizon (Figure 1-2). The telescope is used to collect stray light in a well defined viewing direction with a 1 degree field of view and the integrated concentrations of trace gases along each line of sight: the Slant Column Density (SCD, the product of the gas concentration times the path length in the atmosphere) is derived using non-linear least square fitting of multiple reference spectra. If the instrument is ground-based and the telescope is pointed close to the horizon, the increased path length through the surface layer of the atmosphere makes this technique particularly sensitive to trace gases within the boundary layer because it allows lower concentrations of the gas to be measured with the same SCD[16, 17, 18]. This creates a distinct advantage to probe the marine/coastal boundary layer.

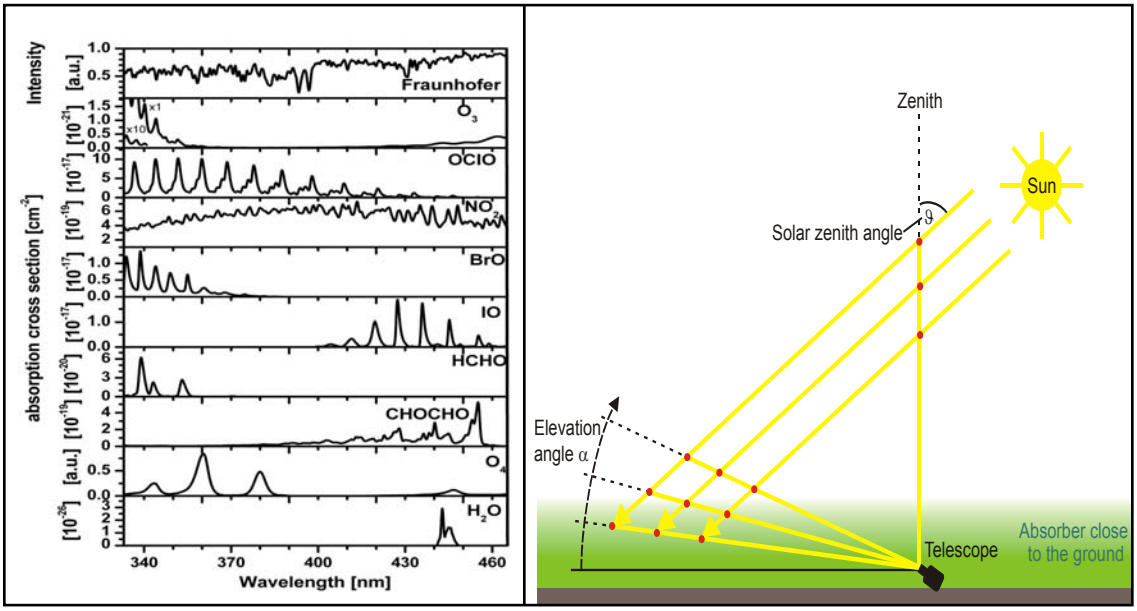

Figure 1-2
Absorption profiles of different atmospheric trace gasses, and schematic sketch of a MAX-DOAS setup.

2
MATERIAL AND METHODS

Outlying Landing Field #8 (OLF)

The Outlying Landing Field #8 (OLF) site is part of the Southeastern Aerosol Research and Characterization (SEARCH) network. SEARCH is an eight-station network initiated by EPRI and several electric utilities in 1998 and located in AL, FL, GA and MS (Figure 2-1). It provides continuous measurements of O_3, NO_2, NO_y, NO, SO_3, SO_2, $PM_{2.5}$, and other air constituents, as well as meteorological parameters such as wind speed and direction, temperature, and humidity. At three stations (OLF, JST, and BHM), Hg^0, RGM, and HgP are also measured. OLF (30.551N, 87.376W, 45 masl) is located 20 km northwest of downtown Pensacola, and 15 km west of the coal-fired power plant Crist. It is adjacent to a quiet road (<100 vehicles/day) and is on the northern end of a large (500 ha) field. Ground cover to the south is short grass to a distance of at least 500m and to the north is brush. I-10 and US-90 run more or less east–west ~1.1 km northeast and 1.6 km south of the site, respectively. Several single-family dwellings are located within 500m. Mercury readings at OLF are taken 5-6 m off the ground every two hours. The readings consist of 12 consecutive five-minute averages for Hg^0 and 1 hour integrated concentrations of HgP (as Hg-$PM_{2.5}$) and RGM. The detection limit for Hg^0 is ~0.1 ng m^{-3}, more than an order of magnitude lower than the background concentration, and for RGM and HgP it is 1.5±0.5 pg m^{-3}.

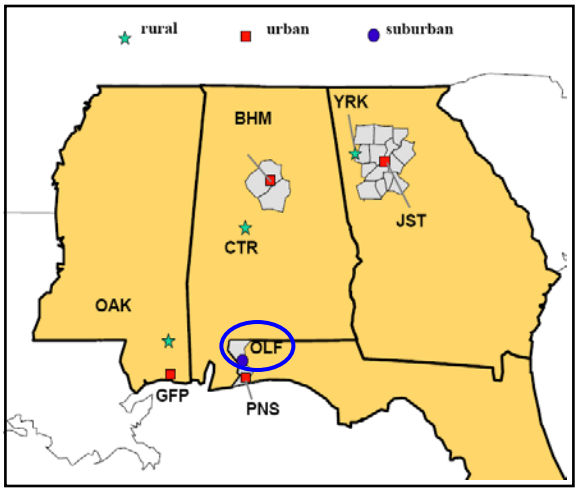

Figure 2-1
SEARCH network sites, with OLF encircled in blue. From: http://www.atmospheric-research.com.

Mini-MAX-DOAS Measurements

In March 2008 the University of Colorado refurbished and deployed a compact MAX-DOAS instrument, known as a Mini-MAX-DOAS system. The instrument was operated remotely until November 2008. The Mini-MAX-DOAS is designed to be a convenient solution for field measurements as all of the components are contained within a single enclosure. It features a commercial Ocean Optics USB2000 spectrometer-detector coupled to a small quartz fiber and a lens mounted to the front of the enclosure. The instrument was modified to be water tight prior to deployment at OLF, the electronics were upgraded, and the telescope was heated slightly to avoid water condensation caused by the high humidity experienced in the Gulf Region, and which would distort the photon light path. The spectral interval observed ranged from 330 to 460 nm. The instrument was operated between March and November 2008; a total of 28847 spectra were collected during 108 days of measurements. All spectra were analyzed for bromine oxide (BrO), iodine oxide (IO), nitrogen dioxide (NO_2), formaldehyde (HCHO), glyoxal (CHOCHO) and oxygen dimers (O_4); 86% of the spectra passed quality assurance.

In this study, one-minute data of nitrogen species (NO, NO_2), ozone, wind speed, and wind direction, as well as the speciated mercury data were used to identify periods of elevated RGM, and constrain a numerical box model of bromine chemistry to assist in the interpretation of the Mini-MAX-DOAS observations. Diurnal profiles for all the complimentary data collected at OLF are shown in the Appendix.

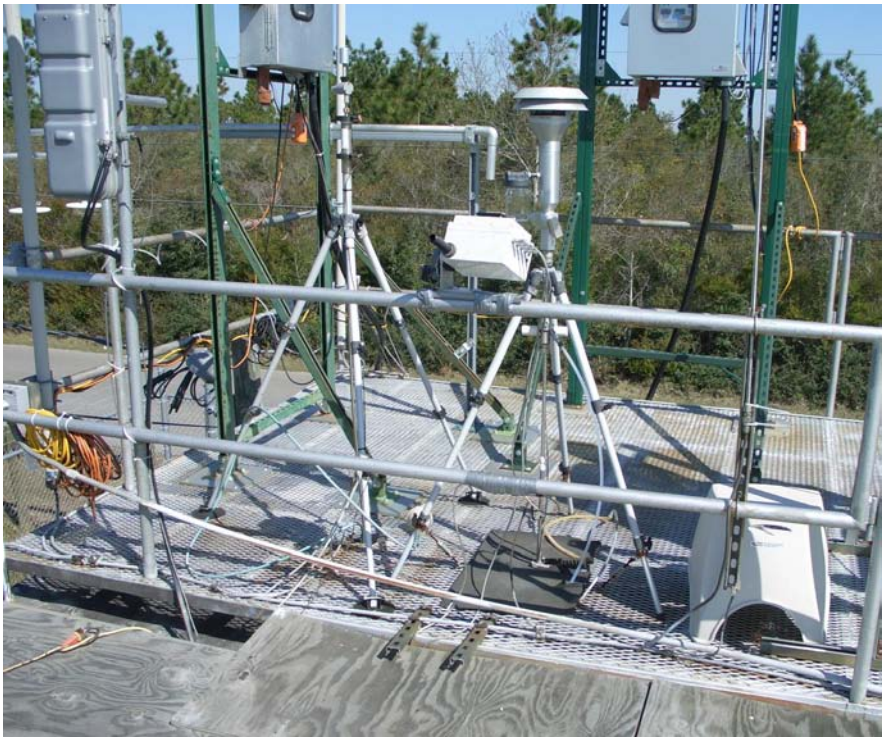

Figure 2-2
Mini-MAX DOAS (white “box” with black telescope) at OLF.

Photochemical Box Model

OVOC are relevant sources of HO_2 radicals that provide additional sink reactions for Br and BrO. The relevance of these sink reactions is demonstrated by means of a photochemical box model that was constructed using reactions (R5) to (R17). The rate parameters were taken from the reference listed on the right, and are given at a temperature of 298K. Bromine chemistry is complex, and the purpose of this model is to illustrate the effect that elevated concentrations of NO_x, HO_x and OVOC have on the partitioning of halogens between reactive and chemically inert reservoir species. Reactions of BrO and Br with NO_x species serve as a reservoir for bromine, and reactions between Br and HO_2 and/or OVOCs produce HBr can be considered an irreversible sink for Br radicals as they effectively remove reactive Br from the atmosphere[19, 20, 21].

(R5)	$Br + O_3 \rightarrow BrO + O_2$	$k_5 = 1.2\text{x}10^{-12}$ $cm^3\ molec^{-1}\ s^{-1}$ [22]
(R6)	$Br + NO_2 \rightarrow BrNO_2$	$k_6 = 2.7\text{x}10^{-11}$ $cm^3\ molec^{-1}\ s^{-1}$ [22]
(R7)	$Br + HCHO \rightarrow HBr$ + products	$k_7 = 1.1\text{x}10^{-12}$ $cm^3\ molec^{-1}\ s^{-1}$ [23]
(R8)	$Br + CHOCHO \rightarrow HBr$ + products	$k_8 = 2.2\text{x}10^{-12}$ $cm^3\ molec^{-1}\ s^{-1}$ [23]
(R9)	$Br + HO_2 \rightarrow HBr + O_2$	$k_9 = 1.7\text{x}10^{-12}$ $cm^3\ molec^{-1}\ s^{-1}$ [22]
(R10)	$BrO + NO \rightarrow Br + NO_2$	$k_{10} = 2.1\text{x}10^{-11}$ $cm^3\ molec^{-1}\ s^{-1}$ [22]
(R11)	$BrO + BrO \rightarrow Br + Br + O_2$	$k_{11} = 2.7\text{x}10^{-12}$ $cm^3\ molec^{-1}\ s^{-1}$ [22]
(R12)	$BrO + h\nu \rightarrow Br + O$	$J_{12} = 2.4\text{x}10^{-2}$ s^{-1} [22]
(R13)	$BrO + NO_2 \rightarrow BrONO_2$	$k_{13} = 1.8\text{x}10^{-11}$ $cm^3\ molec^{-1}\ s^{-1}$ [22]
(R14)	$BrO + HO_2 \rightarrow HOBr + O_2$	$k_{14} = 2.4\text{x}10^{-11}$ $cm^3\ molec^{-1}\ s^{-1}$ [22]
(R15)	$BrNO_2 + h\nu \rightarrow Br + NO_2$	$J_{15} = 3.2\text{x}10^{-3}$ s^{-1} [22]
(R16)	$BrONO_2 + h\nu \rightarrow BrO + NO_2$	$J_{16} = 9.3\text{x}10^{-4}$ s^{-1} [22]
(R17)	$HOBr + h\nu \rightarrow Br + HO$	$J_{17} = 1.5\text{x}10^{-3}$ s^{-1} [22]

3
RESULTS AND DISCUSSION

NO_2, OVOC and halogen oxide data

NO_2 was observed on a regular basis, and column-averaged concentrations exceeded 0.15 ppb in more than 50% of the spectra, with typical concentrations in the ppb concentration range during mornings; concentrations were below the detection limit (0.15 ppb) in the afternoon; similarly, HCHO and CHOCHO concentrations exceeded 0.5 ppb and 0.03 ppt in 36% and 33% of the spectra; typical concentrations are 1.5 ppb and 0.15 ppb respectively. BrO and IO concentrations were below the detection limit (<5 ppt and <2 ppt, respectively) in virtually all spectra, and did not allow a reliable quantification of these gases. The detection limit of the Mini-MAX-DOAS is photon shot-noise limited down to 1σ RMS residual noise levels of $\sim 10^{-3}$, when deviations from pure photon counting statistics are observed with this instrument. In particular, the instrument sensitivity does not improve beyond this threshold when multiple spectra are co-added. This barrier is not a fundamental limitation for the MAX-DOAS technique, and can be overcome with better detectors used in science grade MAX-DOAS instruments.

RGM and Hg^0 data

Figures 3-1 to 3-4 present the diurnal profiles of RGM and Hg^0. RGM measurements are binned by wind speed, and RGM measurements are plotted against wind direction for the entire dataset (March to November 2008) and for data segregated for the three seasons covered within the time frame of this project (spring, summer, and fall). The data shows that diurnal profiles are most prominent during spring and summer and are hardly evident during fall. Plots of RGM data as a function of wind direction show that during a majority of the elevated RGM (>20 pg m^{-3}) events the wind was from the south and fell between 2-6 m s^{-1}. This means that air was being transported from the direction of the Gulf of Mexico to OLF and did not come from other directions with known sources, such as power plant Crist to the east. The decreasing RGM concentrations at wind speeds larger than 6 m s^{-1} at all seasons, though again predominantly during spring and summer, could be due to uptake of RGM in sea salt aerosol. Sea salt forms as the result of bubbles bursting and releasing aqueous salts contained in seawater to the atmosphere; the source strength for sea salt scales with the cube of wind-speed, as indicated by the white-cap ratio. At the time of this writing, the aerosol data from OLF were still being analyzed, and were not available to corroborate this theory. However, several modeling studies suggest that uptake to aerosol is needed to bring lower observations of RGM at elevated wind speeds into agreement with model predictions[24, 25]. The low RGM concentrations at low wind speeds (<2 m s^{-1}) are rather uniformly distributed over all wind directions, and are indicative of background RGM levels. In conclusion, both photochemical as well as meteorological factors determine the RGM concentration in the MBL.

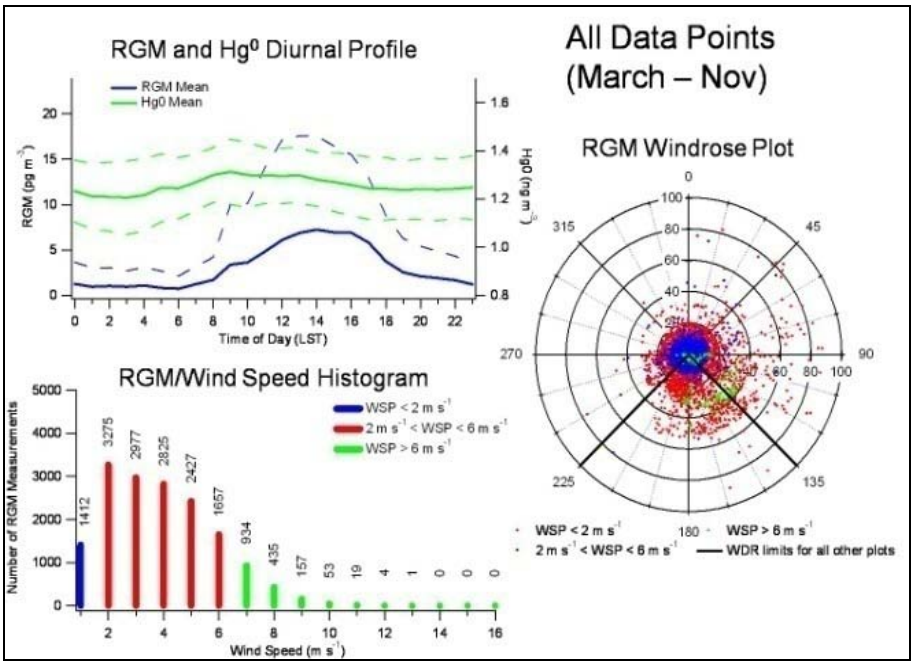

Figure 3-1
Mean diurnal cycle of all RGM and Hg^0 data collected during the entire MAX-DOAS deployment shown in r pper left graph. Dashed lines represent 95% confidence intervals. RGM measurements binned by WSP shown in lower left graph. Plot of RGM vs. WDR (North = 0°, East = 90°, South = 180°, West = 270°) for each binned WSP shown in graph to the right. Circles represent concentrations (pg m^{-3}).

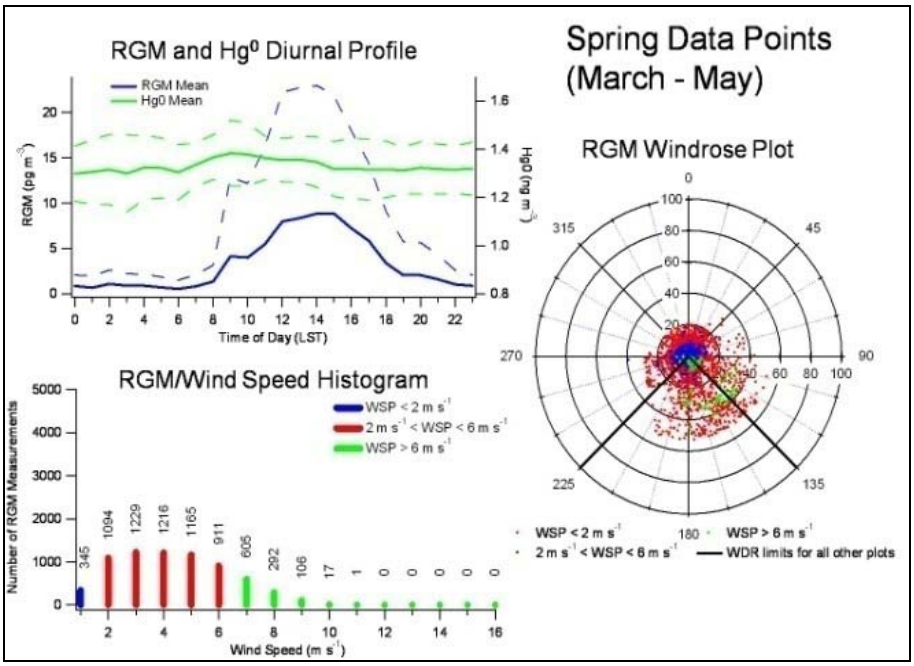

Figure 3-2
Data subsets for data collected during spring.

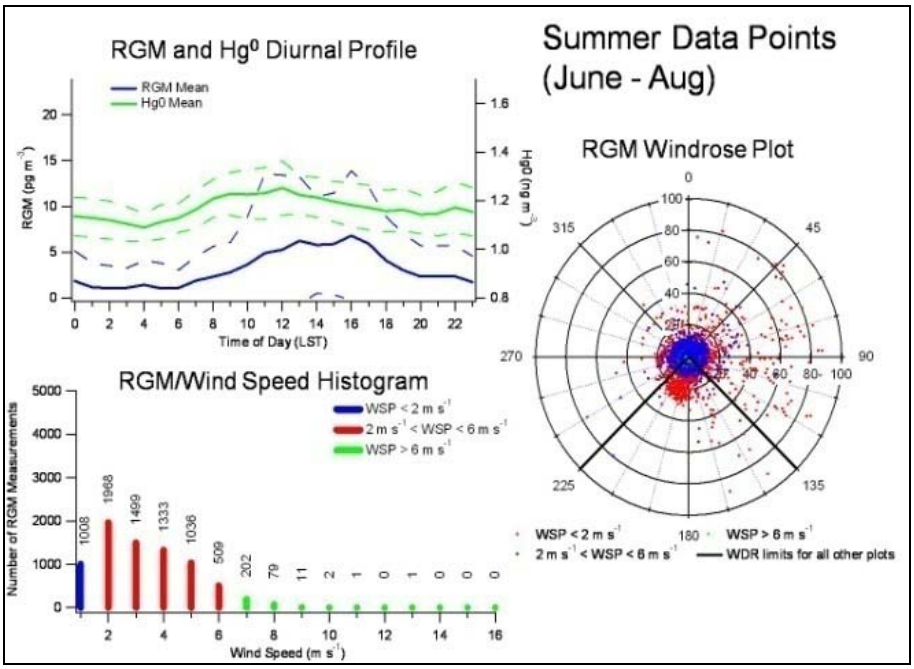

Figure 3-3
Data subsets for data collected during summer.

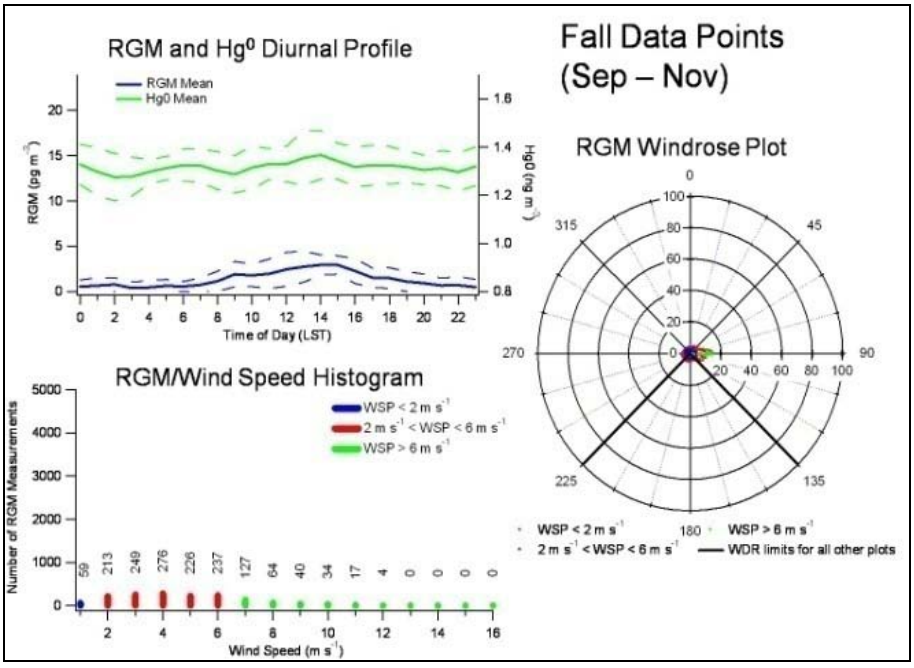

Figure 3-4
Data subsets for data collected during fall.

Halogen Data

The Mini-MAX-DOAS data put an upper limit to concentrations of BrO and IO of <5 ppt and <2 ppt, respectively. While the instrument in principle allows remote sensing of both gases over the open ocean from OLF, the tree line south of OLF limits the extent to which the remote sensing character can be used to observe the marine boundary layer directly. This is because the tree line puts a lower limit of about 2 degrees to the elevation angle. For a one kilometer high boundary layer, this elevation angle corresponds to 28km horizontal fetch, which corresponds to about the distance to the ocean, but is not enough to exclude sources in southerly direction over a substantial portion of the light path. In practice, the dispersion of the Mini-MAX DOAS telescope (1 degree) further increases the lowest angle that can be realized in any measurement strategy. A larger telescope is needed to decrease the dispersion of the telescope and realize lower elevation angles at OLF; raising the telescope to a higher location was considered, but the idea was rejected as the available infrastructure would not be rugged enough to assure accurate knowledge of the elevation angles; and modifications of the available infrastructure were not compatible with the budget of this project.

However, there are also chemical reasons that preclude the detection of BrO at OLF. Sources of NO_x, HO_2 and OVOC are located in southerly direction and lower the concentrations of Br and BrO at OLF as will be illustrated in the following. OLF is located in a semi-rural environment, where NO_x originates from local transportation sources and is transported from Pensacola; point sources can also affect OLF in instances. NO and NO_2 were always present in elevated concentrations; NO_x concentrations exceeded several ppb in the early morning, and was on the order of 0.2 ppb in the afternoon. Typical diurnal profiles for NO and NO_2 are shown in the Appendix, as is the diurnal profile of ozone. The ozone concentrations increased from about 25 ppb during the morning to about 40ppb in the early afternoon, indicating that photochemical ozone formation is not NO_x-limited at OLF. The ozone data thus corroborates the presence of NO_x, which provides an efficient sink for both Br and BrO. The Mini-MAX-DOAS observations of OVOCs like HCHO and CHOCHO are also consistent with VOC-limited ozone production; it indicates the photochemical oxidation of hydrocarbons from biogenic and anthropogenic origin at OLF. HCHO and CHOCHO were observed from all wind directions, indicating that the sources have characteristics of area sources, consistent with the semi rural character of the OLF site that is surrounded by forests and scattered urbanizations.

The box model was initiated with concentrations as listed in Table 3-1, which represent typical concentrations at OLF in the morning and afternoon, high and low NO_x regime, respectively (see Appendix).

Table 3-1
Initial concentrations of all species used in the box model for elevated NO_x and low NO_x concentrations.

Species	Elevated NOx	Low NOx
Br	0.1 ppt	0.1 ppt
BrO	1 ppt	1 ppt
O3	30 ppb	40 ppb
NO	2 ppb	0.15 ppb
NO2	3 ppb	0.7 ppb
HO2	10 ppt	100 ppt
HCHO	1.0 ppb	1.5 ppb
CHOCHO	150 ppt	300 ppt

Figure 3-5 contains the partitioning of bromine between Active Br and its various Br reservoir species, as predicted by the box model for both the low and elevated NO_x scenarios after one hour, corresponding to the transport time of an air parcel from the ocean to OLF assuming a wind speed of 6 m s^{-1}. Additionally, from this data the expected ratio of BrO/Active Br and BrO/Total Br, where Active Br is the sum of Br and BrO and Total Br is the sum of Active Br and all bromine reservoir species, were calculated. These results are illustrated in Table 3-2.

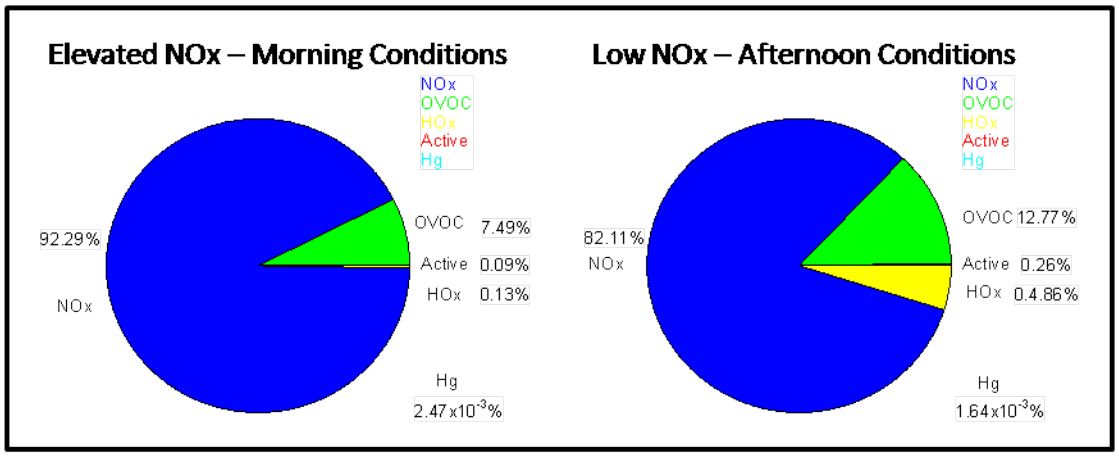

Figure 3-5
Partitioning of bromine into various reservoir species as predicted by the model after one hour for a) the low NO_x and b) the elevated NO_x scenario. Blue indicates NOx related reservoirs ($BrONO_2$, $BrNO_2$); Yellow indicates HO_x related reservoirs and sinks (HOBr, HBr), Green indicates OVOC related reservoirs and sinks (HOBr, HBr). It is assumed here that half the HO_2 originates from OVOC photolysis.

Table 3-2
Expected ratio (1=100%) of BrO/Active Br and BrO/Total Br based on box model calculations.

Ratio	Elevated NOx	Low NOx
BrO/Active Br	0.46	0.885
BrO/Total Br	0.00042	0.0023

These calculations demonstrate that the presence of NO_x, HO_2, and OVOC significantly impact the partitioning of bromine species at OLF, likely causing the concentration of BrO to be lowered by 2-3 orders of magnitude. While it is possible that continued bromine production from airborne sources like sea salt (not represented in the model) might produce active forms of bromine, the concentrations of NO_x, HO_2 and OVOC are still high enough to convert 99% of the active bromine to reservoir species on a time scale of 1 minute. Figure 3-6 demonstrates that despite these sinks, most of the bromine is still present as BrO. The BrO/Br ratio is elevated between 10am and 6pm, and BrO is the primary reservoir of active bromine throughout the day. Interestingly, the modeled BrO/Br ratio shows some correspondence to the diurnal pattern of RGM (Figures 3-1, 3-2, 3-3), although modeled peak levels are reached between 4pm and 6pm, when measured RGM concentrations are actually decreasing. This apparent correspondence could be coincidental; it is generally consistent with our previous conclusion that a combination of photochemical and meteorological (wind speed and wind direction) factors are at the core to explain events of elevated RGM (> 20 pg m^{-3}) levels at OLF.

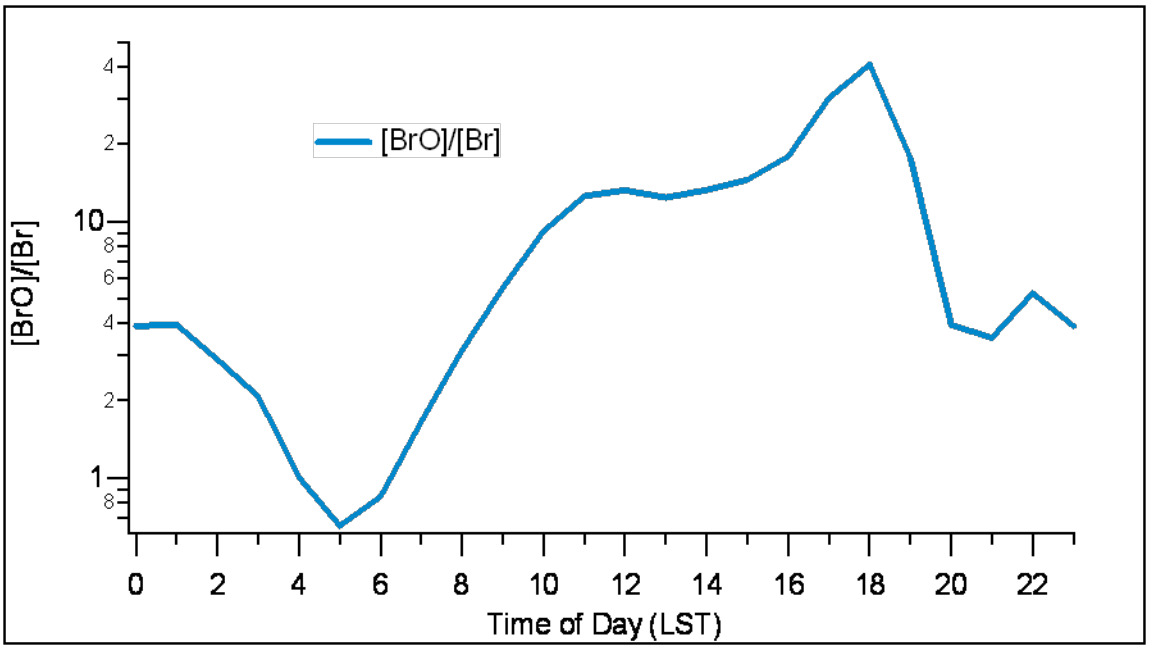

Figure 3-6
The diurnal profile of the [BrO]/[Br] ratio determined from R5 and R10 and using the diurnal profiles of O_3 and NO as measured at OLF (see Appendix).

4
CONCLUSIONS

BrO and IO concentrations were almost always below the detection limit (<5 ppt and <2 ppt, respectively). A numerical box-model revealed that more than 99% of chemically active forms of bromine are converted into chemically inert reservoir species within a minute, i.e. BrO cannot survive transport from the coast to the site, which typically takes about 1hr. Model-predicted BrO/Br ratios show some correspondence with the measured diurnal patterns of RGM, although modeled ratios reached a peak between 4pm and 6pm when measured RGM concentrations are actually decreasing. In addition, the data showed diurnal RGM profiles prominent during spring and summer, and elevated RGM (>20 pg m^{-3}) events were most often observed when the wind was from the south and fell between 2-6 m s^{-1}. Decreasing RGM concentrations at wind speeds larger than 6 m s^{-1} could be due to uptake of RGM in sea salt aerosols. Low RGM concentrations at low wind speeds (<2 m s^{-1}) were observed with winds from all directions, indicating background levels of RGM. Hence, both photochemical as well as meteorological factors determine the concentration of RGM in the MBL. These processes inside the marine boundary layer are important to explain events of elevated RGM levels (> 20 pg m^{-3}) at OLF.

NO_2 was observed on a regular basis, and concentrations exceeded 0.15 ppb in more than 50% of the spectra; similarly, typical HCHO and CHOCHO concentrations were 1.5ppb and 0.15ppb respectively. The data collected and results generated warrant future research. However, OLF is suboptimal for observing halogen oxide radicals because (1) the tree line south of OLF limits the extent to which the remote sensing character of MAX-DOAS could be used to observe the marine boundary layer remotely; (2) sources of NO_x, HO_2 and OVOC are located in southerly direction and preclude the detection of BrO at OLF (concentration lowered by a factor > 100); (3) the detection sensitivity of the Mini-MAX-DOAS instrument is not sufficient to quantify BrO concentrations at OLF. A reliable quantification of halogen oxide radicals near Pensacola, Florida requires a site that is less affected by NO_x, HO_2 and OVOC, and would benefit from a research grade MAX-DOAS instrument. Measurements with a more sensitive instrument are currently underway at an unobstructed site <0.5 miles from the Gulf.

5
REFERENCES

1. Schroeder, W.H.; Munthe, J. Atmospheric Mercury: An Overview. Atmos. Environ., 1998, 32, 809-822.
2. Engle, M.A.; Tate, M.T.; Krabbenhoft, D.P.; Kolker, A.; Olson, M.L.; Edgerton, E.S.; DeWild, J.F.; McPherson, A.K. Characterization and cycling of atmospheric mercury along the central US Gulf Coast. App. Geochem., 2008, 23, 419-437.
3. Liu, G.L.; Cai, Y.; Kalla, P.; Scheidt, D.; Richards, J.; Scinto, L.J.; Gaiser, E.; Appleby, C. Mercury Mass Budget Estimates and Cycling Seasonality in the Florida Everglades. Environ. Sci. Technol., 2008, 42, 1954-1960.
4. Selin, N.E.; Jacoab, D.J.; Yantosca, R.M.; Strode, S.; Jaegle, L.; Sunderland, E.M. Global 3-D land-ocean-atmosphere model for mercury: Present-day versus preindustrial cycles and anthropogenic enrichment factors for deposition. Global Biogeochemical Cycles, 2008, 22, GB2011, doi:10.1029/2007GB003040.
5. Hynes, A.J.; Donohoue, D.L.; Goodsite, M.E.; Hedgecock, I.M. Our current understanding of major chemical and physical processes affecting mercury dynamics in the atmosphere and at air–water/terrestrial interfaces. In Mercury Fate and Transport in the Global Atmosphere; Pirrone, N., Mason, R.P., Eds.; UNEP Global Mercury Partnership; 2008.
6. Ariya, P.A.; Khalizov, A.; Gidas, A. Reactions of Gaseous Mercury with Atomic and Molecular Halogens: Kinetics, Product Studies, and Atmospheric Implications. J. Phys. Chem. A, 2002, 106, 7310-7320.
7. Donohoue, D.L.; Bauer, D.; Cossairt, B.; Hynes, A.J. Temperature and Pressure Dependent Rate Coefficients for the Reaction of Hg with Br and the Reaction of Br with Br: A Pulsed Laser Photolysis-Pulsed Laser Induced Fluorescence Study. J. Phys. Chem. A, 2006, 110, 6623-6632.
8. Tossell, J.A. Calculation of the Energetics for Oxidation of Gas-Phase Elemental Hg by Br and BrO. J. Phys. Chem. A, 2003, 107, 7804-7808.
9. Pal, B.; Ariya, P.A. Studies of ozone initiated reactions of gaseous mercury: kinetics, product studies, and atmospheric implications. Phys. Chem. Chem. Phys., 2004, 6, 572 – 579.
10. Lindberg, S.; Bullock, R.; Ebinghaus, R.; Engstrom, D.; Feng, X.B.; Fitzgerald, W.; Pirrone, N.; Prestbo, E.; Seigneur, C A Synthesis of Progress and Uncertainties in Attributing the Sources of Mercury in Deposition. Ambio, 2007, 36, 19-32.
11. Steffen, A.; Douglas, T.; Amyot, M.; Ariya, P.; Aspmo, K.; Berg, T.; Bottenheim, J.; Brooks, S.; Cobbett, F.; Dastoor, A.; Dommergue, A.; Ebinghaus, R.; Ferrari, C.; Gardfeldt, K.; Goodsite, M.E.; Lean, D.; Poulain, A.J.; Scherz, C.; Skov, H.; Sommar, J.; Temme, C. A synthesis of atmospheric mercury depletion event chemistry in the atmosphere and snow. Atmos. Chem. Phys., 2008, 8, 1445-1482.

12. Lindberg, S.E.; Brooks, S.; Lin, C.J.; Scott, K.J.; Landis, M.S.; Stevens, R.K.; Goodsite, M.; Richter, A. Dynamic Oxidation of Gaseous Mercury in the Arctic Troposphere at Polar Sunrise. Environ. Sci. Techn., 2002, 36, 1245-1258.

13. Peleg, M.; Matveev, V.; Tas, E.; Luria, M. Mercury Depletion Events in the Troposphere in the Mid-Latitudes at the Dead Sea, Israel. Environ. Sci. Technol., 2007, 41, 7280-7286.

14. Honninger, G.; Leser, H.; Sebastian, O.; Platt, U. Ground-based measurements of halogen oxides at the Hudson Bay by active longpath DOAS and passive MAX-DOAS. Geophys. Res. Lett., 2004, 31, L04111, doi:10.1029/2003GL018982.

15. Wagner, T.; Ibrahim, O.; Sinreich, R.; Frieb, U.; von Glasow, R.; Platt, U. Enhanced tropospheric BrO over Antarctic sea ice in mid winter observed by MAX-DOAS on board the research vessel Polarstern. Atmos. Chem Phys., 2007, 7, 3129-3142.

16. Sinreich, R.; Volkamer, R.; Filsinger, F.; Kern, C.; Platt, U.; Sebastian, O.; Wagner, T. MAX-DOAS measurement of Glyoxal during ICARTT-2004. Atmos. Chem. Phys. 2007, 7, 1293-1303.

17. Honninger, G.; Platt, U. Observations of BrO and its vertical distribution during surface ozone depletion at Alert. Atmos. Env., 2002, 36, 2481-2489.

18. Honninger, G.; von Friedeburg, C.; Platt, U. Multi axis differential optical absorption spectroscopy (MAX-DOAS). Atmos. Chem. Phys., 2004, 4, 231-254.

19. Platt, U.; Honninger, G. The role of halogen species in the troposphere. Chemosphere, 2003, 52, 325-338.

20. Wayne, R.P.; Poulet, G.; Biggs, P.; Burrows, J.P.; Cox, R.A.; Crutzen, P.J.; Hayman, G.D.; Jenkin, M.E.; Le Bras, G.; Moortgat, G.K.; Platt, U.; Schindler, R.N. Halogen Oxides: Radicals, sources and reservoirs in the laboratory and in the atmosphere. Atmos. Environ., 1995, 29, 2677-2881.

21. Platt, U.; Janssen, C. Observation and Role of the Free Radicals NO3, ClO, BrO, and IO in the Troposphere. Faraday Discuss., 1995, 100, 175-198.

22. Atkinson, R.; Baulch, D.L.; Cox, R.A.; Crowley, J.N.; Hampson, R.F.; Hynes, R.G.; Jenkin, M.E.; Rossi, M.J.; Troe, J. Evaluated kinetic and photochemical data for atmospheric chemistry: Volume III – gas phase reactions of inorganic halogens. Atmos. Chem. Phys., 2007, 7, 981-1191.

23. Sander, R.; Crutzen, P.J. Model study indicating halogen activation and ozone destruction in polluted air masses transported to the sea. J. Geophys. Res., 1996, 101, 9121-9138.

24. Selin, N.; Jacob, D.J.; Park, R.J.; Yantosca, R.M.; Strode, S.; Jaegle, L.; Jaffe, D. Chemical cycling and deposition of atmospheric mercury: Global constraints from observations. J. Geophys. Res., 2007, 112, D02308, doi:10.1029/2006JD007450.

25. Holmes, C.D.; Jacob, D.J.; Mason, R.P.; Jaffe, D.A. Sources and deposition of reactive gaseous mercury in the marine atmosphere. Atmos. Environ., 2009, 43, 2278-2285.

A
APPENDIX

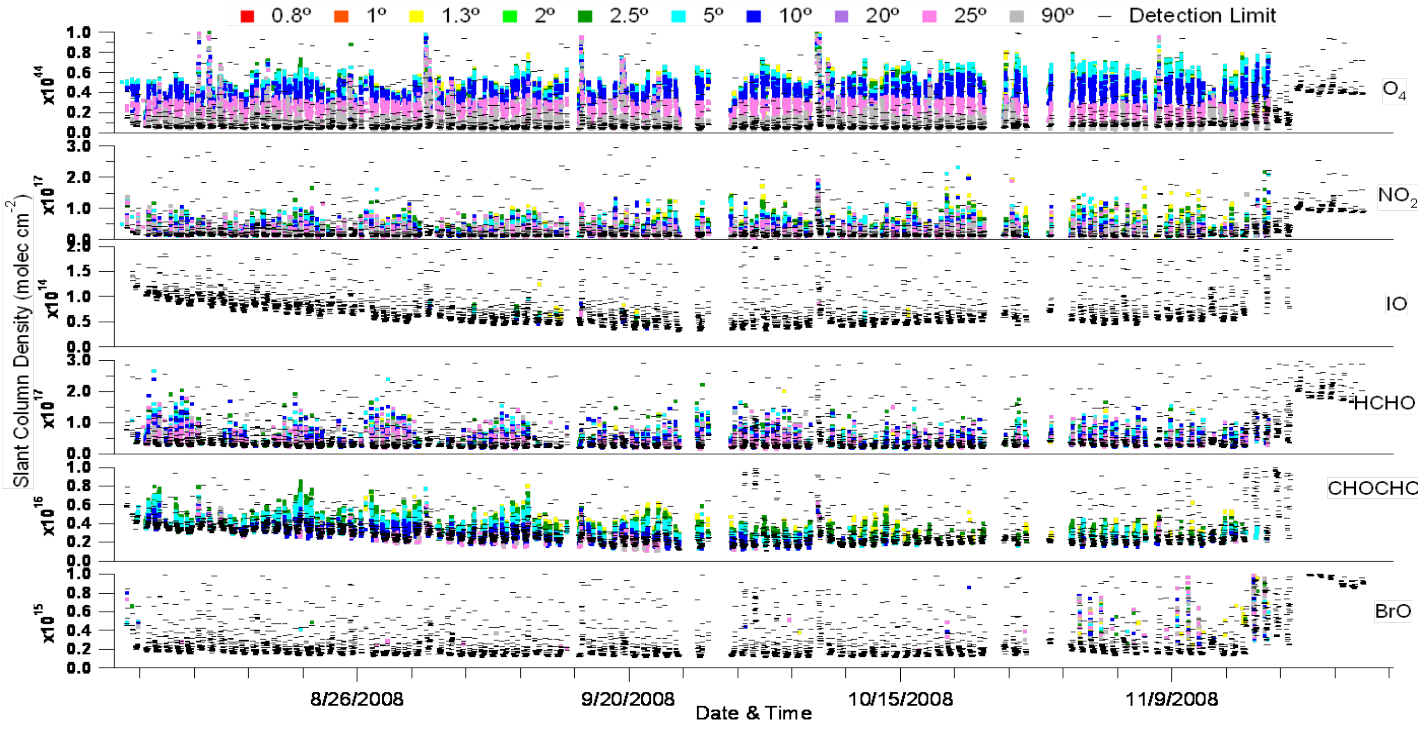

Figure A-1
Time series plots of O_4, NO_2, IO, HCHO, CHOCHO, and BrO dSCDs, respectively, as measured from the Mini-DOAS instrument over the time period of March – November 2008. The black lines for each of the plots represent the average detection limit for that trace gas over the time period.

Mean diurnal profiles of the supplementary data collected at OLF, based on all date collected during MAX-DOAS operations.

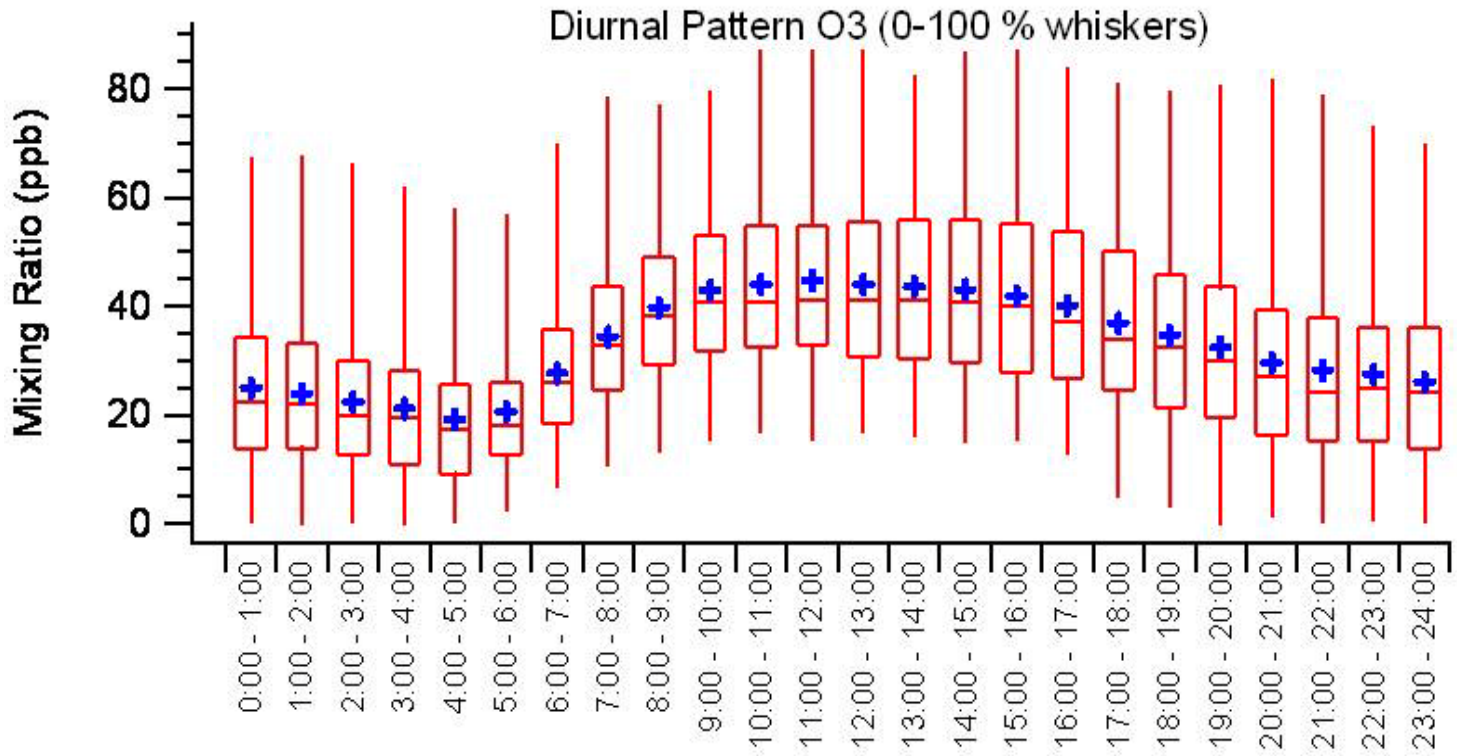

Figure A-2
Whisker plots of diurnal profiles for O_3, NO, NO_2, precipitation, and CO, respectively, measurements of which were part of the supplementary data provided for OLF.

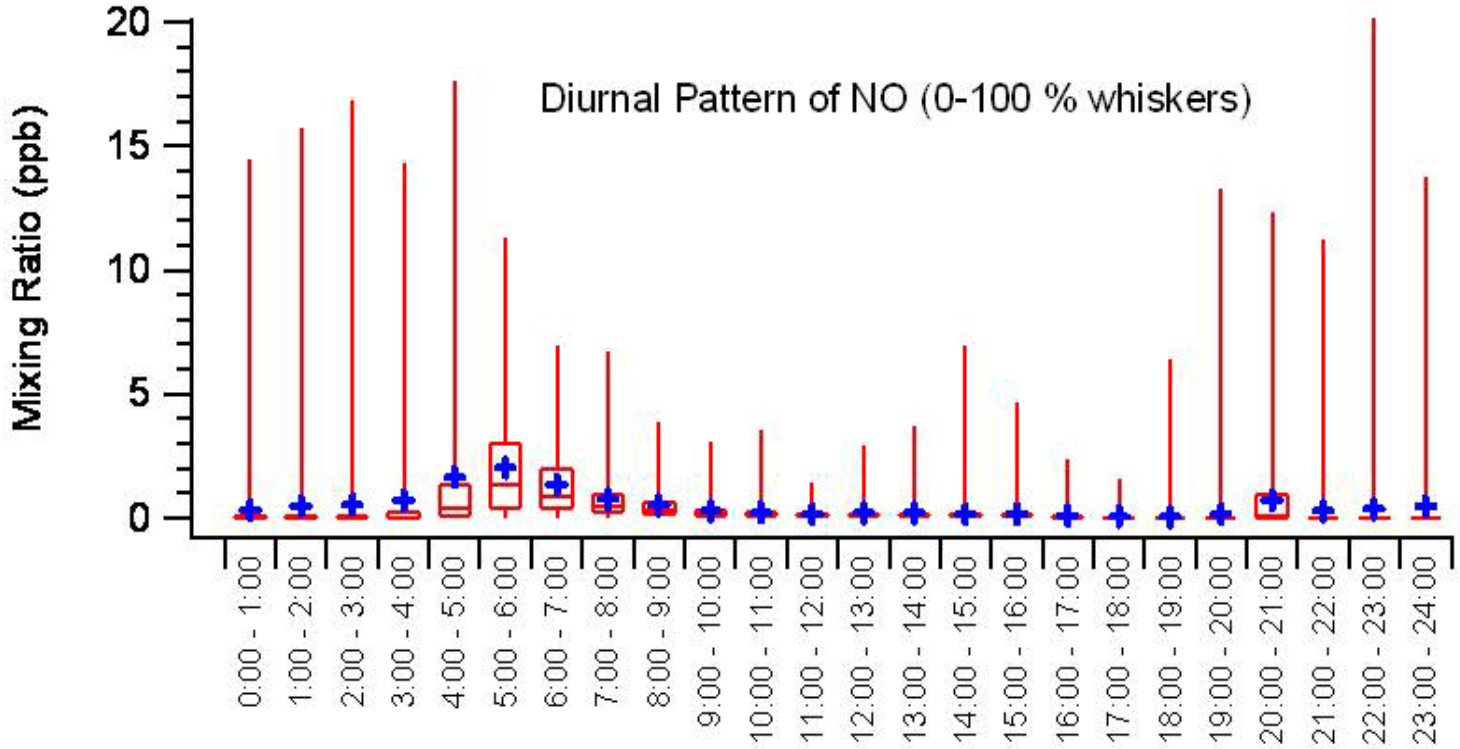

Figure A-2 (continued)
Whisker plots of diurnal profiles for O_3, NO, NO_2, precipitation, and CO, respectively, measurements of which were part of the supplementary data provided for OLF.

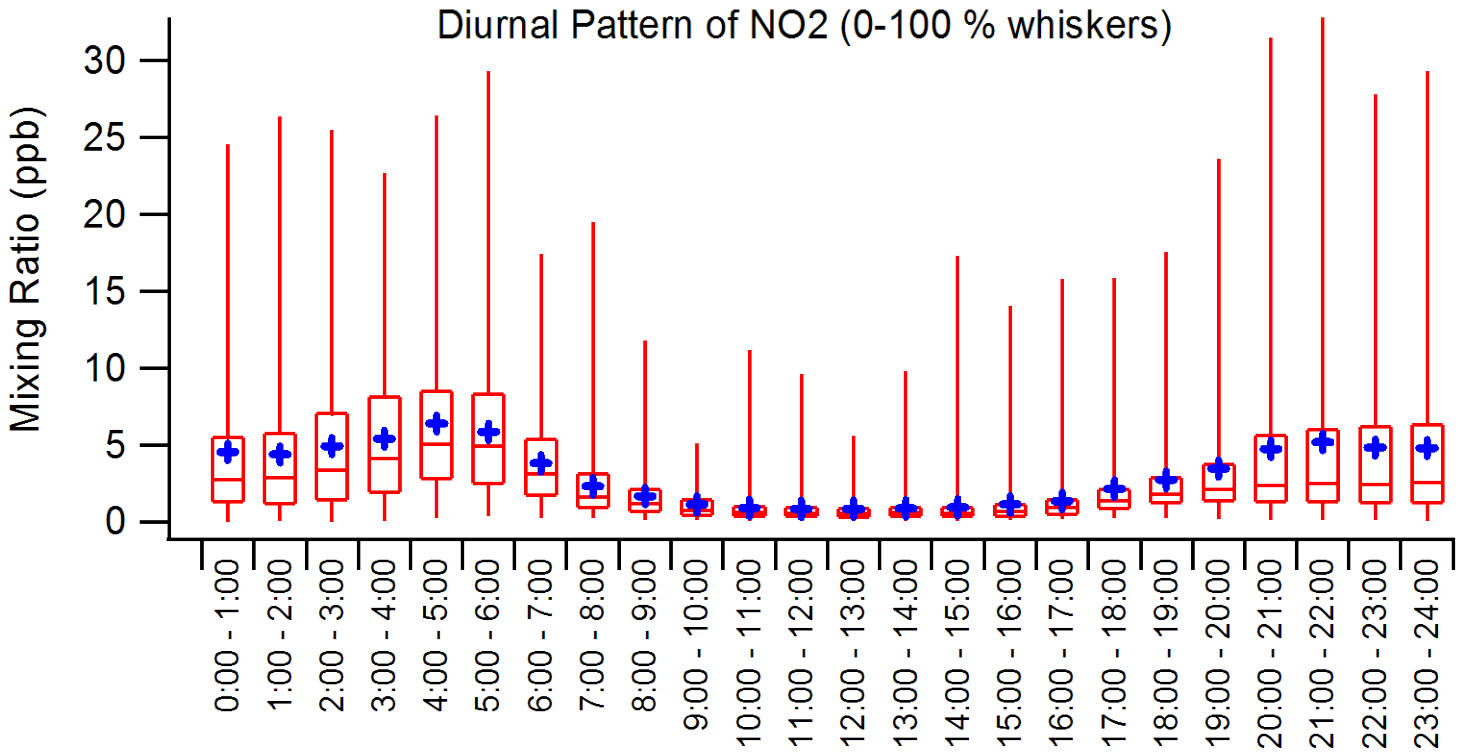

Figure A-2 (continued)
Whisker plots of diurnal profiles for O_3, NO, NO_2, precipitation, and CO, respectively, measurements of which were part of the supplementary data provided for OLF.

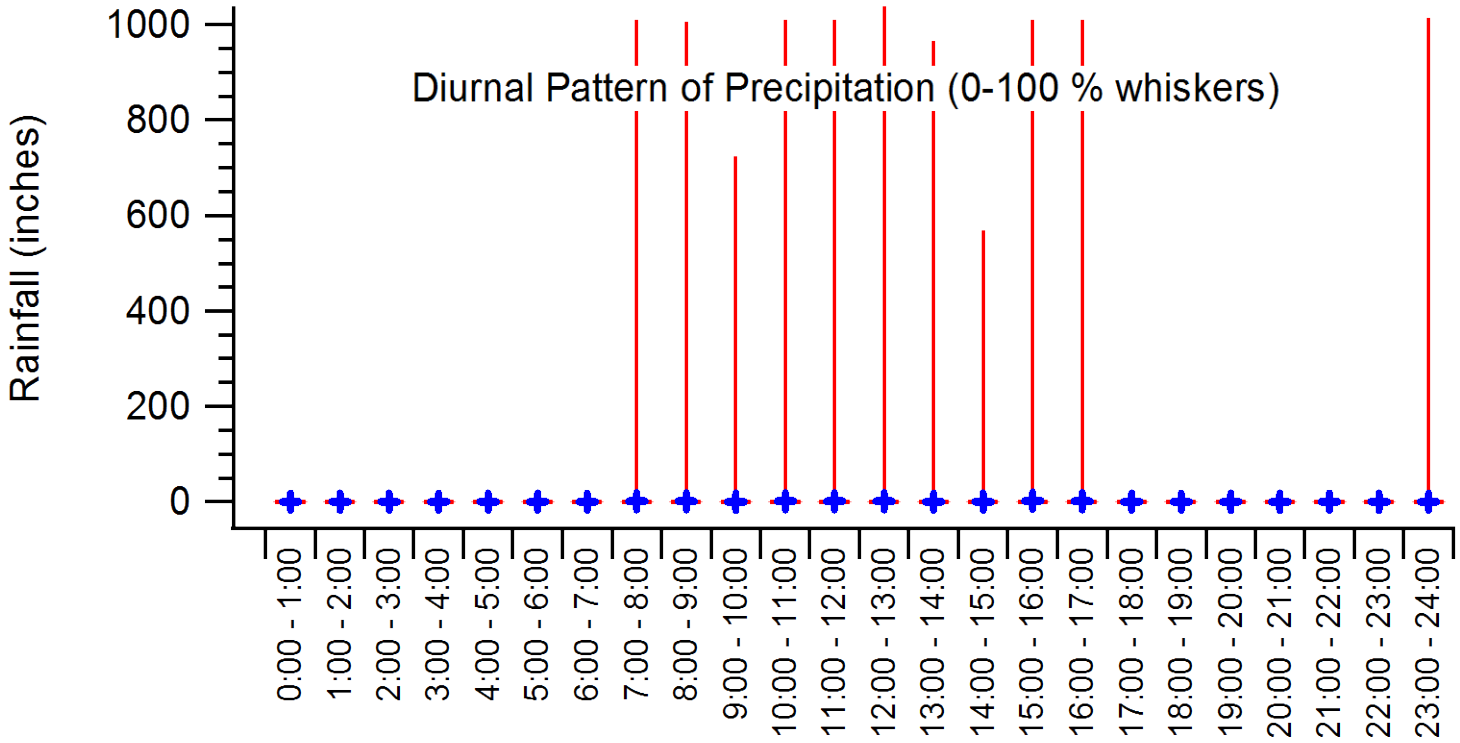

Figure A-2 (continued)
Whisker plots of diurnal profiles for O_3, NO, NO_2, precipitation, and CO, respectively, measurements of which were part of the supplementary data provided for OLF.

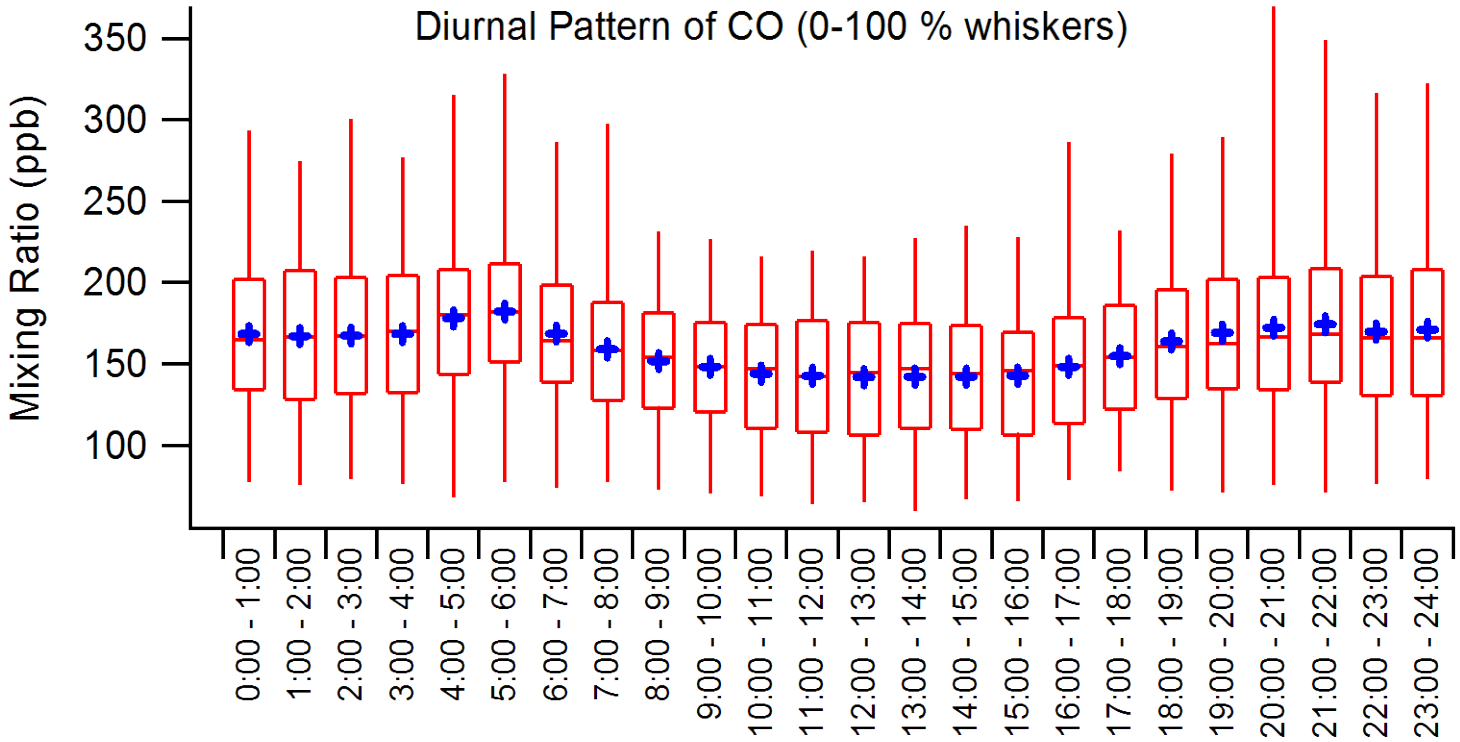

Figure A-2 (continued)
Whisker plots of diurnal profiles for O_3, NO, NO_2, precipitation, and CO, respectively, measurements of which were part of the supplementary data provided for OLF.

Export Control Restrictions

Access to and use of EPRI Intellectual Property is granted with the specific understanding and requirement that responsibility for ensuring full compliance with all applicable U.S. and foreign export laws and regulations is being undertaken by you and your company. This includes an obligation to ensure that any individual receiving access hereunder who is not a U.S. citizen or permanent U.S. resident is permitted access under applicable U.S. and foreign export laws and regulations. In the event you are uncertain whether you or your company may lawfully obtain access to this EPRI Intellectual Property, you acknowledge that it is your obligation to consult with your company's legal counsel to determine whether this access is lawful. Although EPRI may make available on a case-by-case basis an informal assessment of the applicable U.S. export classification for specific EPRI Intellectual Property, you and your company acknowledge that this assessment is solely for informational purposes and not for reliance purposes. You and your company acknowledge that it is still the obligation of you and your company to make your own assessment of the applicable U.S. export classification and ensure compliance accordingly. You and your company understand and acknowledge your obligations to make a prompt report to EPRI and the appropriate authorities regarding any access to or use of EPRI Intellectual Property hereunder that may be in violation of applicable U.S. or foreign export laws or regulations.

The Electric Power Research Institute Inc., (EPRI, www.epri.com) conducts research and development relating to the generation, delivery and use of electricity for the benefit of the public. An independent, nonprofit organization, EPRI brings together its scientists and engineers as well as experts from academia and industry to help address challenges in electricity, including reliability, efficiency, health, safety and the environment. EPRI also provides technology, policy and economic analyses to drive long-range research and development planning, and supports research in emerging technologies. EPRI's members represent more than 90 percent of the electricity generated and delivered in the United States, and international participation extends to 40 countries. EPRI's principal offices and laboratories are located in Palo Alto, Calif.; Charlotte, N.C.; Knoxville, Tenn.; and Lenox, Mass.

Together...Shaping the Future of Electricity

Program:

Technology Innovation

1019522

Electric Power Research Institute
3420 Hillview Avenue, Palo Alto, California 94304-1338 • PO Box 10412, Palo Alto, California 94303-0813 USA
800.313.3774 • 650.855.2121 • askepri@epri.com • www.epri.com